Short Course
Detectors for Small-Animal SPECT

(with emphasis on scintillation detectors)

Harrison H. Barrett

Center for Gamma-Ray Imaging

The University of Arizona
Tucson Arizona

NIBIB

Outline

- Detector resolution and other specs
- Modular cameras and integrating detectors
- Scintillator materials and statistics
- Optical coupling
- Photodetectors
- CCD/CMOS-based gamma cameras
- MLE in scintillation cameras
- Likelihood theory and camera design
- Summary and conclusions

Detector resolution

Conventional wisdom: Detector resolution is irrelevant since you are always limited by the collimator anyway

Spatial resolution with a collimator

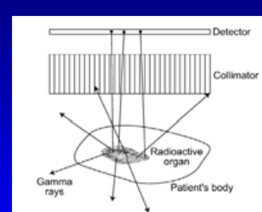

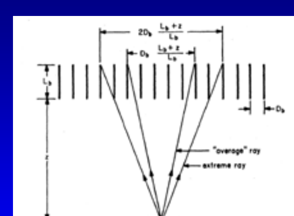

$$\delta_{phc} \approx D_b \frac{L_g + L_b + z}{L_b}$$

$$\delta_{tot}^2 = \delta_{phc}^2 + \delta_{det}^2$$

Sensitivity *gain* with high-resolution detectors

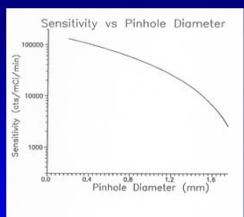

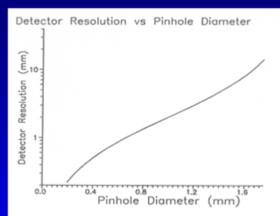

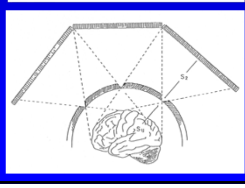

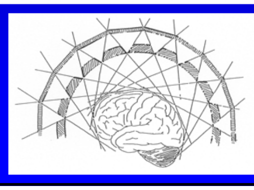

Trading detector resolution for counts

8 mm resolution
3.2M counts

6 mm resolution
400k counts

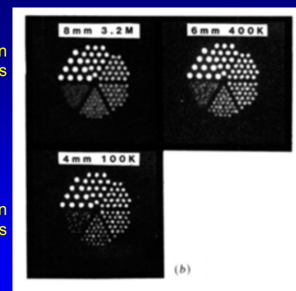

4 mm resolution
100k counts

Improving resolution 2X allows 32X *reduction* in counts for same subjective image quality

Gerd Muehllehner,
Phys. Med. Biol. (30)2:163-173, (1985).

System resolution and lesion detectability

10X *reduction* in pinhole area → 10X *increase in* human-observer detectability in a nonuniform background

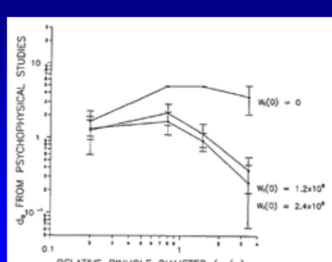

Uniform background

Nonuniform background

J. Rolland and H. H. Barrett
J. Opt. Soc. Am. A, 9:649-658 (1992)

Morals of the story

- Improved detector resolution can be traded for improved *sensitivity* in SPECT
- Key Parameter: Detector space-bandwidth product

Sp-BW = (Area of detector) / (Area of PSF)
= Area of detector × 2D bandwidth .

Need for high detection efficiency?

In both SPECT and PET, objective performance measures improve with better system resolution, even at the expense of counts

Useful single-number characterization for detectors:

Space-bandwidth-efficiency product
(coincidence efficiency for PET)

Count-rate capability
Do we need fast detectors?

- No – we can use lots of slower ones
- We can even use integrating detectors!

Modular detectors

- Modular detectors are:
  - Electrically and mechanically independent
  - Relatively low cost
  - Small (compared to object size)
- Advantages:
  - Inexpensive
  - Easily interchanged for service
  - Reconfigurable for different imaging applications
  - High countrate capability
  - Parallel collection of projection data, high sensitivity

Examples of modular detectors

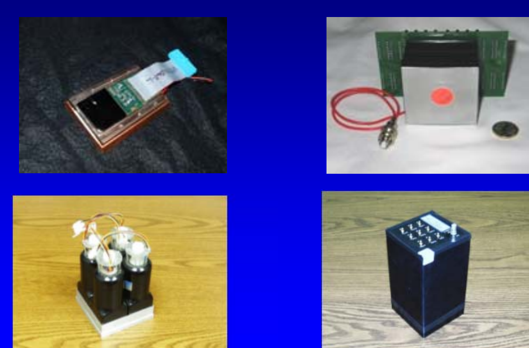

Photon counting and energy resolution with integrating detectors

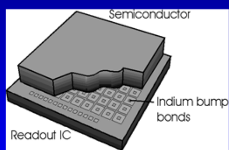

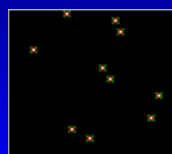

Barber et al., Physica Medica, 1993; Trans. Med. Imag. 1993

A scintillation camera consists of:

- Scintillator material
  - Monolithic crystal
  - Segmented crystal
  - Columnar
- Optical coupling mechanism
  - Proximity coupling ("light guide" in an Anger camera)
  - Lenses and mirrors
  - Fiber optics
- Optical sensors
  - PMTs
  - MAPMTs, PSPMTs
  - Si PIN diodes, APDs, SPMs, etc.
  - CCD or CMOS sensors
- Data processing
  - Event detection
  - Anger arithmetic
  - ML methods

Scintillators

- Key requirements for scintillation cameras:
  - Large crystals
  - High light output
  - Good proportionality
  - Low Fano factor!

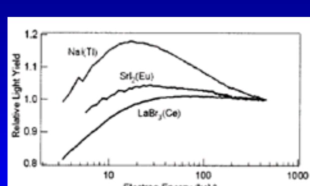

Cherepy et al.,

Nonproportionality degrades energy *and* spatial resolution
(Correlated signals reduce Fisher information)

Candidate scintillators for SPECT

Material	Density (g/cm^3)	Attenuation coefficient @140keV (cm^{-1})	Light yield (phot/MeV)	Peak emission (nm)	Non-Proportionality (10-200 keV)
NaI(Tl)	3.67	2.64	45,000	415	20%
$LaBr_3$(Ce)	5.1	2.89	74,000	375	15%
SrI_2(Eu)	4.6	3.28	90,000	435	5%
YI_3(Ce)	4.6	3.44	99,000	549	<2%
LuI_3(Ce)	5.6	6.16	115,000	522	< 2%
Elpasolites	4.2	3.95	Up to 60,000	445	< 2%

Energy resolution and nonproportionality

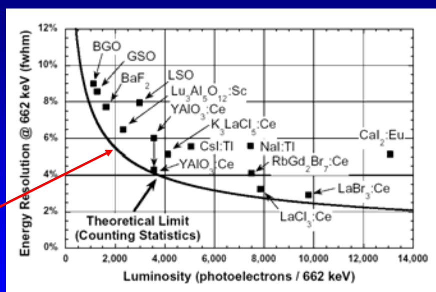

Poisson limit
F=1

W. Moses, Nuclear Instruments and Methods in Physics Research A 487 (2002) 123–128

What everyone knows about Fano Factor:

$$\sigma_n^2 = \bar{N}_{opt}\eta F$$

But it is also true (Barrett and Swindell, 1981) that:

$$\langle \Delta n_1 \Delta n_2 \rangle = \eta_1 \eta_2 \bar{N}_{opt}(F-1)$$

So Fano factor can be measured by observing correlations in two different photodetectors viewing the same scintillation event.

Positive correlations are caused by:
F > 1
Multiple energy deposition pathways + nonproportionality
Variation of light collection as function of random position
Random energy deposition, other nuisance parameters
PMT gain noise, electronic noise
Negative correlations are caused by
F < 1
Photon anti-bunching, sub-Poisson (sub-Moses) statistics

Experimental Setup for measurement of Fano factors for scintillation materials

A. Bousselham, H. H. Barrett, V. Bora, K. Shah, *Nucl. Instrum. Meth. A.*, 620, 359-362, 2010.

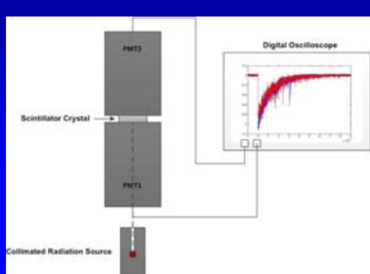

19

SrI_2:Eu

- High light output (100,000 photons /MeV)
- Good energy resolution (3% @ 662 KeV)
- Ideal candidate!

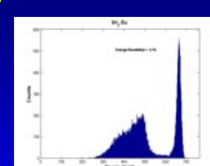

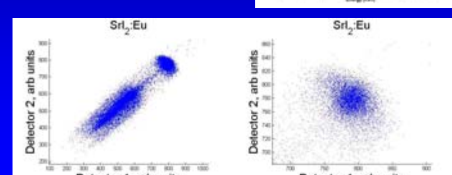

20

YAP:Ce

•Low light output (18,000 photons / MeV)
•Good energy resolution (4.4% @ 662 KeV)

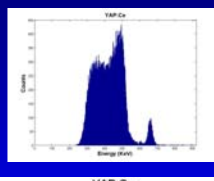

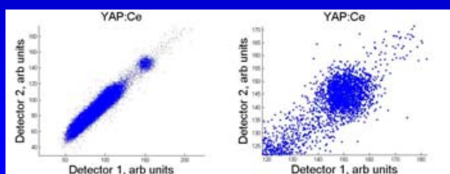

CsI:Na

•High light output (43000 photons /MeV)
•Bad energy resolution (6%)

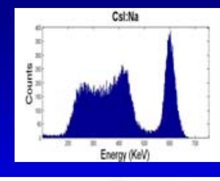

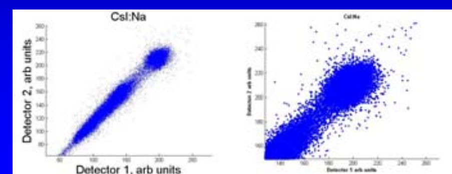

Estimates of Fano factor

Unpublished work of Vaibhav Bora et al.

Crystal	Correlation coefficent	Photoelectron Fano factor (F_n)	Photon Fano Factor (F_N)
SrI_2:Eu	-0.3336 ± 0.2384	0.7324 ± 0.0604	0.0441 ± 0.2157
YAP:Ce	0.1036 ± 0.0691	1.1237 ± 0.0042	1.4419 ± 0.0151
CsI:Na	0.3643 ± 0.2292	1.6132 ± 0.1960	3.1899 ± 0.6999
$LaBr_3$:Ce	-0.32 ± 0.17	0.72 ± 0.06	0.10 ± 0.16

Optical coupling in Scintillation cameras

Proximity coupling (Anger-like designs)

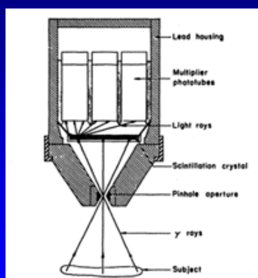

The original Anger camera

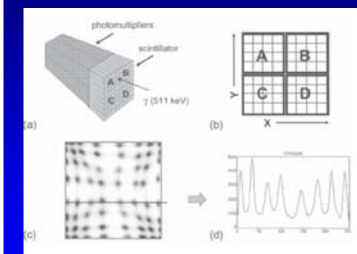

PET block detector

Imaging optics: lenses and fibers

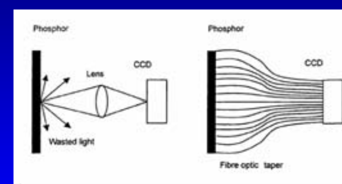

Fiber optic tapers

Schott Glass

Roper Scientific

The demagnification problem

Both lenses and fiber tapers have numerical apertures

Collection efficiency varies as m^2 for both
(m = magnification; usually m < 1)

Large FOV + small CCD => small coupling efficiency

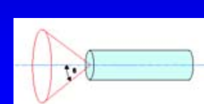

Seeing the light (optical sensors)

- Photomultiplier tubes
  - Conventional
  - Multi-anode (MAPMT)
  - Position-sensitive (PSPMT)
- Photodiodes
  - Si PiN
  - Silicon drift detectors
  - HgI_2
  - Avalanche photodiodes (APDs)
  - Geiger-mode APD arrays (SPMs)
- CCD and CMOS sensors

Advances in Photocathodes

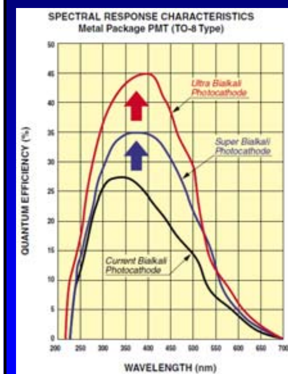

Hamamatsu

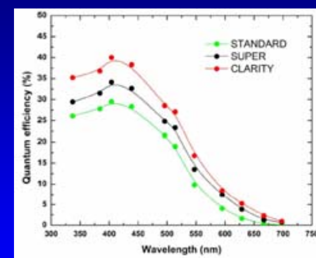

Photonis

Multianode PMTs and SPM arrays

Hamamatsu H8500 MAPMT

SensL SPM array

PMTs: Pluses and minuses

- Pluses
  - Familiar technology
  - Large gain before electronic noise
  - Modest (but improving) quantum efficiency
  - Dark current negligible (with blue scintillators)
  - Large sensor size (reduces processing req)
- Minuses
  - Bulky, fragile
  - Gain depends on voltage, temperature, time
  - Sensitive to magnetic fields
  - Large sensor size (affects spatial and DOI resol)

Silicon photodiodes: Pluses and minuses

- Pluses
  - High quantum efficiency
  - Long-wavelength sensitivity
  - Stable, robust
  - Small sensor size
- Minuses
  - No gain before electronic noise
  - Dark current
  - Small sensor size

Avalanche Photodiodes (APDs) and Silicon Photomultipliers (SPMs, Geiger-mode APDs): Pluses and minuses

- Pluses
  - High quantum efficiency
  - Internal gain before electronic noise
  - Small sensor size (potentially high spatial resolution)
- Minuses
  - Noisy gain (APDs)
  - Gain depends strongly on voltage (APDs)
  - Low fill factor partially negates QE advantage (SPMs)
  - Small sensor size (costly to cover large area)

Recent advances in CCDs

- Larger sensor area
  - Less light loss
- Back-thinning and AR coating
  - Higher QE
- Cooling
  - Lower dark current
- Electron multiplication
  - Smaller read noise (at expense of dynamic range)
- Parallel readout
  - Shorter frame time

CCD	Kodak KAF-09000
Array Size (pixels)	3056 x 3056
Pixel Size	12 x 12 microns
Imaging Area	36.7 x 36.7 mm (1345 mm2)
Imaging Diagonal	51.9 mm
Video Imager Size	3.24"
Linear Full Well (typical)	110K electrons
Dynamic Range	84 dB
QE at 400 nm	37%
Peak QE (550 nm)	64%
Anti-blooming	>100X

Dark current:
0.04e^- /sec @ - 40 c

Readout noise: 7e^- @ 1 MHz

Effect of back-thinning

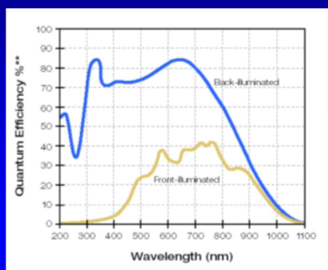

Leica M-Monochrom

Rangefinder CCD

Recent advances in CMOS (active pixel) sensors

- Signal processing circuitry at each pixel
- Greatly reduced readout noise at high pixel rates
- Microlenses to concentrate light on active area
- “Digital” lenses (telecentric in image space)
- Larger sensors
- Parallel readout
- Ultrafast frame rates

“Prosumer” DSLR cameras

24 X 36 mm CMOS sensors

Nikon D700, 12 MP, ~$2400

Canon EOS 5D Mk II, 22 MP, ~ $2500
Canon EOS 5D, 12 MP, ~ $2000

Two new sCMOS cameras from Andor

CMOS chip layout

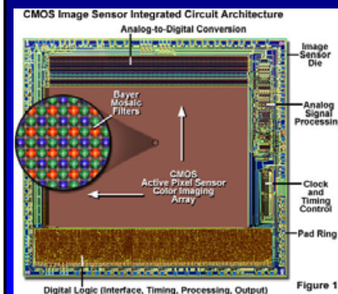

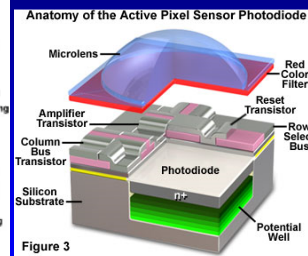

http://micro.magnet.fsu.edu/primer/digitalimaging/cmosimagesensors.html

Microlenses

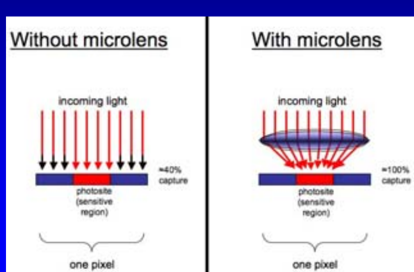

A digital lens

Nikon parallel readout and pipeline processing

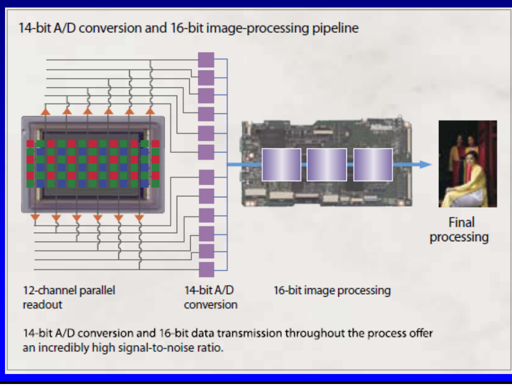

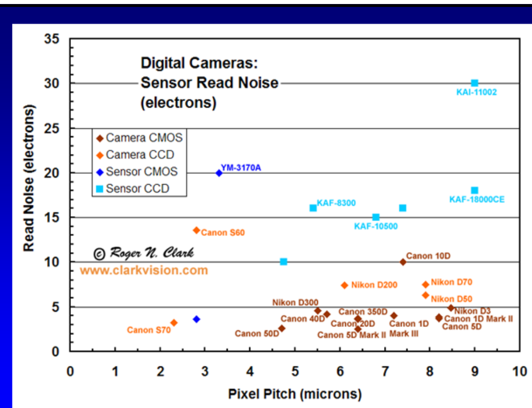

http://www.clarkvision.com/imagedetail/digital.sensor.performance.summary/

CCD/CMOS-based scintillation cameras
Photon counting with integrating detectors

- Lens-coupling to scientific-grade CCD
  - LumiSPECT (Taylor 2004, Miller 2007)
- Image intensification
  - EMCCD (DeVree 2004, Nagarkar 2005, Teo 2006, Miller 2006, Lewis 2007)
  - Microchannel plates (Miller 2006)
  - Vacuum intensifier + EMCCD (Meng 2006)

LumiSPECT
Sean Taylor (2004)

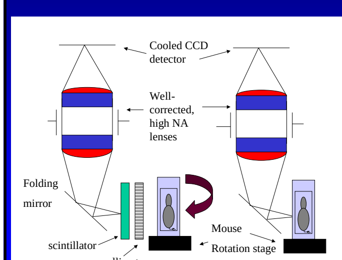

Gamma-Converter

Columnar CsI(Tl)

Parallel-hole collimator

LumiSPECT CCD properties

Detector Type	VersArray 1300B, scientific grade
CCD Format	$1340 \times 1340 \times 20\mu m$ Pixels
Dark Current	$0.1e^{-}$/pixels/sec@$-40^{o}C$, $0.5e^{-}$pixels/hr@$-110^{o}C$
Read Noise	$3e^{-}$@50kHz scan rate, $12e-$@1MHz scan rate
Binning Modes	$2 \times 2, 3 \times 3, 4 \times 4$
Full-frame Readout	36sec@50kHz, 1.8sec@1MHz
Thermal Precision	± 0.1 degrees Celsius over entire temperature range
Nonuniformity	$\leq 4\%$ over active area of CCD

LumiSPECT Photon-Counting Mode

Brian Miller, 2007

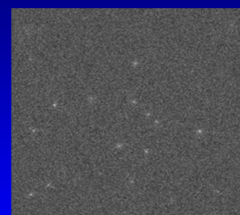
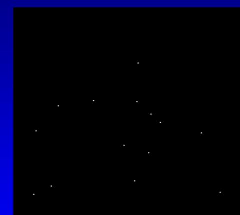

- 2x2 binning to sample at 40μm pixels
- Tc99m γ-rays
- RMD columnar CsI(Tl), 270μm thick

EMCCD-based "Ultra Gamma Camera"

Beekman et al., 2004

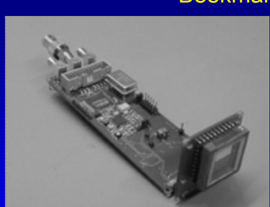

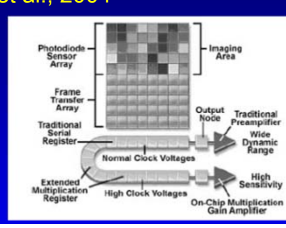

11.5 X 8.6 mm sensor
30 μm X 20 μm pixel

Vacuum intensifier (demagnifier tube) plus EMCCD

L. J. Meng (2006)

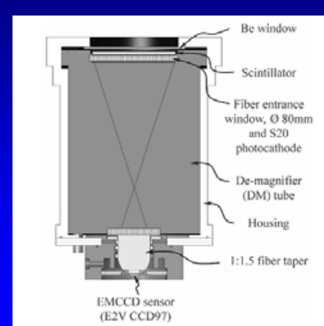

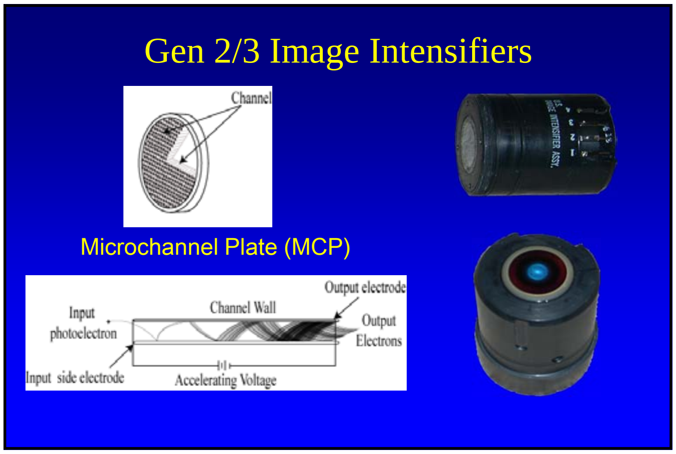
Gen 2/3 Image Intensifiers
Channel
Microchannel Plate (MCP)
Output electrode
Input
photoelectron
Channel Wall
Output
Electrons
Input side electrode
Accelerating Voltage

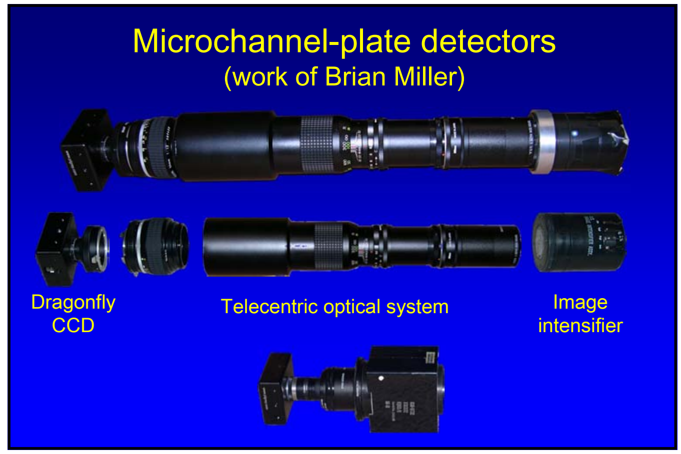
Microchannel-plate detectors
(work of Brian Miller)
Dragonfly
CCD
Telecentric optical system
Image
intensifier

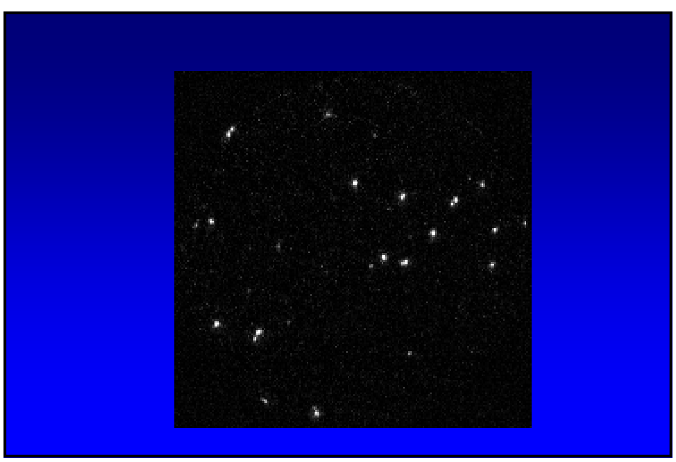

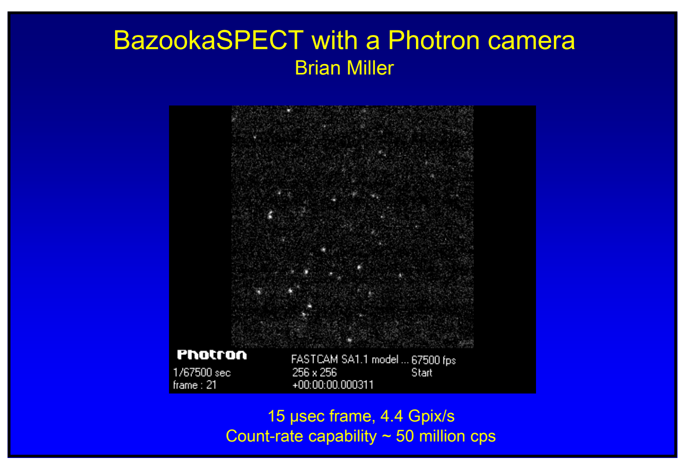
BazookaSPECT with a Photron camera
Brian Miller
Photron
FASTCAM SA1.1 model ... 67500 fps
1/67500 sec
256 x 256
Start
frame : 21
+00:00:00.000311
15 µsec frame, 4.4 Gpix/s
Count-rate capability ~ 50 million cps

Data acquisition and processing for scintillation detectors

- Conventional approach:
  - Immediately apply Anger arithmetic
  - Patch up the problems that result
- Recommended approach:
  - Collect all possible data in list mode
  - Apply rigorous ML estimation methods

Maximum-likelihood estimation

Likelihood = probability (data | parameters)

Maximum likelihood: choose the parameter values that maximize the likelihood for the observed data

Advantages

Accounts for data statistics

Enforces agreement with data in a statistical sense

Nice asymptotic properties (as you get better data)
Best possible variance
Unbiased (right answer on average)

Maximum-likelihood estimation

- MLE maximizes the probability of the data given the parameter :

$$\hat{\boldsymbol{\theta}}_{\mathrm{ML}} \equiv \underset{\boldsymbol{\theta}}{\operatorname{argmax}} \; \mathrm{pr}(\mathbf{g}|\boldsymbol{\theta})$$

- Equivalently, maximizes the logarithm of this conditional probability:

$$\hat{\boldsymbol{\theta}}_{\mathrm{ML}} = \underset{\boldsymbol{\theta}}{\operatorname{argmax}} \; \ln[\mathrm{pr}(\mathbf{g}|\boldsymbol{\theta})]$$

Fisher information matrix

Definition

$$F_{jk} = \left\langle \left[\frac{\partial}{\partial \theta_j} \ln \mathrm{pr}(\mathbf{g}|\boldsymbol{\theta}) \right] \left[\frac{\partial}{\partial \theta_k} \ln \mathrm{pr}(\mathbf{g}|\boldsymbol{\theta}) \right] \right\rangle_{\mathbf{g}|\boldsymbol{\theta}}$$

Cramer-Rao lower bound (for unbiased estimator)

$$\mathrm{Var}\{\hat{\theta}_n\} \geq \left[\mathbf{F}^{-1}\right]_{nn}$$

Off-diagonal elements of inverse relate to covariances of estimates

An *efficient estimator* is one that is unbiased and for which the CR bound become an equality

In any problem, the ML estimator is efficient if an efficient estimator exists

The ML estimator is always asymptotically efficient ...

... as you get more or better data

....thereby increasing the (Fisher) information content

Log-likelihood and FIM for Poisson statistics

$$\ln \Pr(\mathbf{g}|\boldsymbol{\theta}) = \sum_{m=1}^{M} \{-\overline{g}_m(\boldsymbol{\theta}) + g_m \ln[\overline{g}_m(\boldsymbol{\theta})] - \ln g_m!\}$$

$$F_{jk} = \sum_{m=1}^{M} \frac{1}{\overline{g}_m(\boldsymbol{\theta})} \frac{\partial \overline{g}_m(\boldsymbol{\theta})}{\partial \theta_j} \frac{\partial \overline{g}_m(\boldsymbol{\theta})}{\partial \theta_k}$$

Key point: likelihood and FIM can be computed from knowledge of mean data only

Independent Gaussian noise (usual model for electronic noise)

$$\ln \mathrm{pr}(\mathbf{g}|\boldsymbol{\theta}) = constant - \frac{1}{2\sigma^2} \sum_{m=1}^{M} [g_m - \overline{g}_m(\boldsymbol{\theta})]^2$$

$$F_{jk} = \frac{1}{\sigma^2} \sum_{m=1}^{M} \frac{\partial \overline{g}_m(\boldsymbol{\theta})}{\partial \theta_j} \frac{\partial \overline{g}_m(\boldsymbol{\theta})}{\partial \theta_k}$$

Again, log-likelihood and FIM can be computed from knowledge of mean data only

ML Methods for processing signals from gamma-ray detectors

H. H. Barrett et al.,
IEEE Trans. Nucl. Sci., 56:725-735, 2009.

Event-by-event gamma-ray imaging

- Why gamma-ray photons are different from optical photons:
  - Gamma-ray photons arrive at slow rate, compared to resolving time of electronics
  - Large energy per photon
  - Get a lot of information from each photon
- From one photon, can estimate up to five attributes:
  - 2D position on detector face (x, y)
  - Depth of interaction (z)
  - Energy
  - Time of arrival

2D position estimation for a 3X3 modular camera

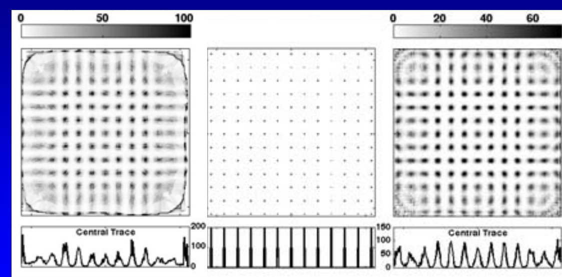

Anger arithmetic (centroid estimation)

13X13 Point grid

ML estimation

ML estimation of 3D interaction position in a monolithic PET detector

Simulations by William Hunter (IEEE MIC 2007)

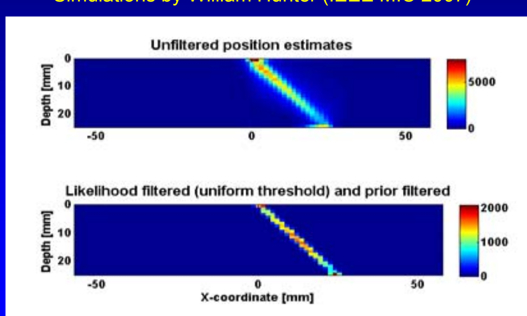

Experimental validation

Work of Stephen Moore (IEEE MIC 2007)

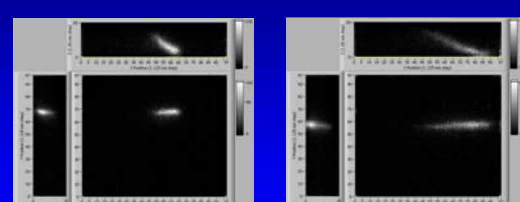

Cramer-Rao bound on 3D estimation performance in a monolithic PET camera

W.C.J. Hunter et al. *IEEE Trans. Nucl. Sci.* 56:189-196, 2009

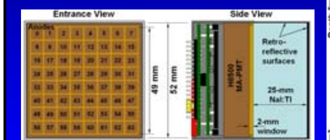

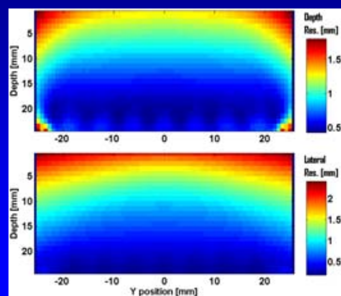

Contracting-Grid Search Algorithm

Example for position estimation for a single experimental event:

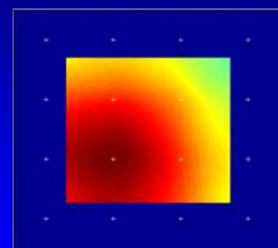

1. "Zero" pad area around detector
2. Evaluate log-likelihood of data at 4 × 4 grid of test locations
3. Select highest likelihood location as center of new grid with half spacing
4. Repeat steps 2 and 3 for fixed number of iterations (6 for CGRI modular gamma camera)

L. Furenlid et al., 2005

J. Hesterman et al., *IEEE Trans.Nucl. Sci.*, 57(3), 1077-1084 2010

ML position estimation in practice

Jacob Hesterman, Luca Caucci, Steve Moore

- Modeling and calibration
  - Optics
  - Poisson noise
  - PMT gain noise
  - Nonproportionality
- Hardware
  - Cell processors
  - GPUs
  - Gate arrays
- Software
  - Native cell processing
  - CUDA
  - Gate array programming

2D position estimation, 9-PMT ModCam: ~ 10^6 events/sec on one PlayStation 3

3D position estimation, 64-anode MAPMT: ~64,000 events/sec on one GeForce 9800

Statistics of scintillation detectors based on CCD or CMOS cameras:

A case study in detector design

B. W. Miller et al., Proc. SPIE, 7450-24, 2009

CCD/CMOS-based scintillation cameras

Photon counting with integrating detectors

- Lens-coupling to scientific-grade CCD
  - LumiSPECT (Taylor 2004, Miller 2007)
- Image intensification
  - EMCCD (DeVree 2004, Nagarkar 2005, Teo 2006, Miller 2006, Lewis 2007)
  - Microchannel plates + CMOS (Miller 2006)
  - Vacuum intensifier + EMCCD (Meng 2006)

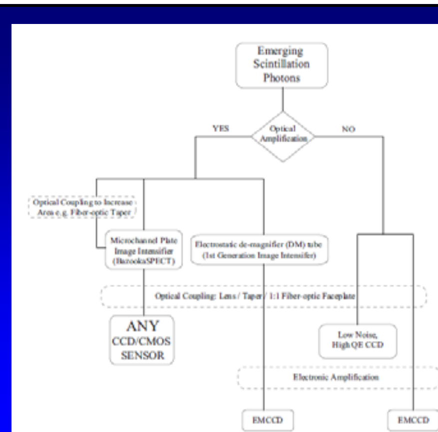

Random effects in this class of gamma cameras

- Random light collection and production of photoelectrons
- Dark current
- Random amplification
- Readout noise after the amplification

Mean signal

Mean number of optical photons produced by gamma photon of energy $\mathcal{E}$:

$$\overline{N}_{opt} = A\mathcal{E}\,,$$

The mean number of electrons generated in the m^{th} pixel;

$$\overline{n}_m(x,y,z,\mathcal{E}) = A\,\mathcal{E}\,\eta_{QE}\,\eta_m(x,y,z) + \overline{n}_m^{dark}\,,$$

where $\overline{n}_m^{dark}$ is the mean number generated in the dark by thermal excitation and $A\,\mathcal{E}\,\eta_{QE}$ is the mean number generated by the scintillation flash.

Mean of the final pixel value g_m:

$$\overline{g}_m(x,y,z,\mathcal{E}) = \overline{G}\,\overline{n}_m(x,y,z,\mathcal{E})$$

where $\overline{G}$ is the overall mean gain, including all components between the photon-to-electron conversion and the final readout.

Variance and covariance

The variance, conditional on the interaction location and energy, is given by

$$\mathrm{Var}\{g_m|x,y,z,\mathcal{E}\} = \overline{n}_m(x,y,z,\mathcal{E})\left[\mathrm{Var}\,G + \overline{G}^2\right] + \sigma^2\,,$$

where $\mathrm{Var}\,G$ is the variance of the gain and σ^2 is the variance of the readout noise, both assumed independent of m.

If the optical blur is negligible compared to pixel size, then the covariance matrix for $\mathbf{g}$, denoted $\mathbf{K}$, has elements given by

$$K_{mm'}(x,y,z,\mathcal{E}) = \left[\overline{n}_m(x,y,z,\mathcal{E})\overline{G}^2(1+\alpha) + \sigma^2\right]\delta_{mm'}\,,$$

where $\alpha \equiv \mathrm{Var}\,G/\overline{G}^2$.

In practice, $\alpha \approx 1$ for both image intensifiers and EMCCDs.

If pre-readout gain is large enough, readout noise is negligible in all systems

Likelihood and log-likelihood

If we approximate the Poisson distribution for n_m by a Gaussian and assume that both the gain noise and the readout noise are Gaussian, the likelihood function is

$$\mathrm{pr}(\mathbf{g}|x,y,z,\mathcal{E}) = \frac{1}{\sqrt{(2\pi)^M \prod_{m=1}^M K_{mm}(x,y,z,\mathcal{E})}} \exp\left\{-\frac{1}{2}\sum_{m=1}^M \frac{[g_m - \overline{g}_m(x,y,z,\mathcal{E})]^2}{K_{mm}(x,y,z,\mathcal{E})}\right\}$$

and the corresponding log-likelihood becomes

$$\ln \mathrm{pr}(\mathbf{g}|x,y,z,\mathcal{E}) = -\frac{1}{2}\sum_{m=1}^M \ln K_{mm}(x,y,z,\mathcal{E}) - \frac{1}{2}\sum_{m=1}^M \frac{[g_m - \overline{g}_m(x,y,z,\mathcal{E})]^2}{K_{mm}(x,y,z,\mathcal{E})} + C\,,$$

where C is a constant, independent of the parameters to be estimated.

Fisher information matrix and Cramér-Rao Bound

$$F_{jj'}(\boldsymbol{\theta}) \approx \frac{1}{1+\alpha}\sum_{m=1}^M \frac{1}{\overline{n}_m(\boldsymbol{\theta})}\frac{\partial \overline{n}_m(\boldsymbol{\theta})}{\partial \theta_j}\frac{\partial \overline{n}_m(\boldsymbol{\theta})}{\partial \theta_{j'}}\,.$$

$$\mathrm{Var}\left\{\hat{\theta}_j\right\} \geq \left[\mathbf{F}^{-1}(\boldsymbol{\theta})\right]_{jj}\,.$$

$$F_{jj'}(\boldsymbol{\theta}) \approx \frac{1}{1+\alpha}\sum_{m=1}^M \frac{1}{\overline{n}_m(\boldsymbol{\theta})}\frac{\partial \overline{n}_m(\boldsymbol{\theta})}{\partial \theta_j}\frac{\partial \overline{n}_m(\boldsymbol{\theta})}{\partial \theta_{j'}}$$

$$\overline{n}_m(x,y,z,\mathcal{E}) = A\,\mathcal{E}\,\eta_{QE}\,\eta_m(x,y,z) + \overline{n}_m^{dark}$$

- Mean gain unimportant, if it is large enough to override readout noise
- Gain noise reduces Fisher information ~ 2x
- Dark current reduces Fisher information
- Dark current can be reduced by use of:
  - cooling
  - photocathode with no red response
  - faster frame rate
- Effect of dark current is reduced by more efficiently creating photoelectrons: larger QE, better optical coupling, larger PC, etc.
- MLE reduces effect of dark current by optimal weighting of pixels
- Demagnification before photocathode is deleterious

Property	Unintensified CCD	EMCCD	Vacuum II + EMCCD	MCP + CMOS
QE	Outstanding	Excellent	Good	Good
Optical collection efficiency	Poor if minification is used	Poor if minification is used	Excellent with large-area intensifier and no minification	Good to excellent, depending on area
Readout noise	Fair, reduced by slow readout (much better with CMOS DSLRs)	Negligible at high gain, but at sacrifice of dynamic range	Same as EMCCD	Negligible, no sacrifice of dynamic range
Dark current	Problematical at room temp, can be reduced by cooling	Same as CCD	Same as CCD	Fair with surplus night vision devices, excellent with custom PC, reduce with high frame rates
Readout speed	Limited by CCD, very poor for scientific CCDs	Limited by EMCCD, ~30 fps	Limited by EMCCD, ~30 fps	Can use ultrafast CMOS, to 67,500 fps

Conclusions

- Space-bandwidth is our most important product
- What Poisson limit?
- Count on integrating detectors
- Are CCDs obsolete?
- Likely, fast and accurate!
- Get more information!